Organic LETTERS

Letter

pubs.acs.org/OrgLett

Zwitterionic N_2O_2-Type Protonated Dipyrrin Bearing a Phosphate Anionic Moiety as a pH-Responsive Fluorescence Indicator

Masaki Yamamura, Hiroyuki Takizawa, and Tatsuya Nabeshima*

Graduate School of Pure and Applied Sciences and Tsukuba Research Center for Interdisciplinary Materials Science (TIMS), University of Tsukuba, 1-1-1 Tennodai, Tsukuba, Ibaraki 305-8571 Japan

Supporting Information

ABSTRACT: Zwitterionic protonated-dipyrrin **1** bearing a phosphate unit was synthesized from the N_2O_2-type tetradentate dipyrrin ligand. Compound **1** is in equilibrium with the deprotonated form **1′** with a pK_a value of 5.8. Compound **1** exhibited a pH-responsive fluorescence under physiological conditions; the fluorescence intensity increased in aqueous media as the pH increased. In living cells, **1** also exhibited emission responsive to pH. Thus, **1** should be applicable as a pH probe for detecting tumor cells.

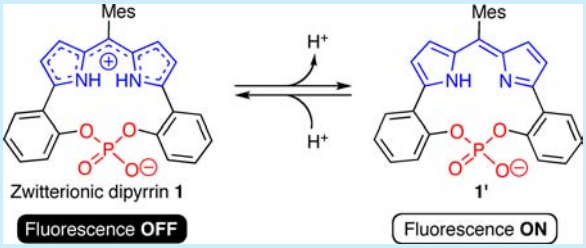

Many fluorescence probes have been developed as powerful tools for studying intracellular functions in living tissues.[1] The pH change in living cells frequently regulates biological processes, such as endocytosis.[2] In addition, special events in living cells, such as cell growth[3] or canceration,[4] are accompanied by a pH change. Thus, fluorescence probes responsive to intracellular pH are applicable to many biological or medical research studies, for example, tumor detection.[5,6] The development of highly sensitive, chemically and photochemically stable, and low-energy excited fluorescence probes is still important and challenging.

Dipyrrins and their complexes are very applicable fluorophores because of their intense absorption and fluorescence properties and excellent photostability.[7,8] We have reported the various complexes of the N_2O_2-type tetradentate dipyrrin ligands.[9,10] One of the most important features of our complexes is their strong luminescence in the red and near-infrared (NIR) regions because such luminescent dyes are very useful for biological applications because of the low emission background and high transparency of biological tissues and living cells in the NIR region.[11] Very recently, Jiang and his colleagues reported dipyrrin-phosphorus complexes,[12] which are highly soluble in water. We have now synthesized a zwitterion of the N_2O_2-type dipyrrin by formation of the phosphate ester, which works as a water-soluble fluorescence probe responsive to the environmental pH.

The reaction of the dipyrrin ligand **L** with phosphoryl chloride in the presence of *N*,*N*-diisopropylethylamine gave the protonated dipyrrin **1** bridged with a phosphate moiety in 74% yield (Scheme 1).

The X-ray crystallographic analysis revealed that **1** does not have any countercation or anion. The dipyrrin moiety is apparently distorted; the dihedral angle between the two pyrrole rings is 32° (Figure 1). Neutral dipyrrin units are usually planar because of the intramolecular hydrogen bond, N−H···N.[13] The distortion of **1** suggests that the protonated structure of the dipyrrin causes repulsion between the two N−H groups. The phosphorus atom has a distorted tetrahedral geometry (∠O−P−O = 90.11(5)−121.06(6)°). The bond distances between the phosphorus and two oxygen atoms, O3

Scheme 1

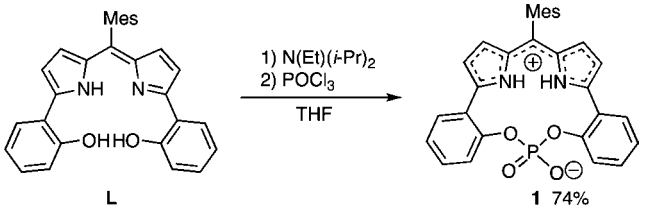

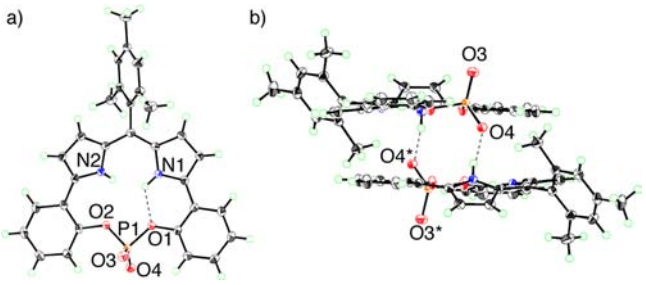

Figure 1. Crystal structure of **1** (50% probability), top (a) and side (b) view. Selected bond lengths (Å) and angles (deg): P(1)−O(1), 1.6375(10); P(1)−O(2), 1.6212(10); P(1)−O(3), 1.4668(10); P(1)−O(4), 1.4781(10); O(1)−P(1)−O(2), 90.11(5); O(2)−P(1)−O(3), 111.30(6); O(3)−P(1)−O(4), 121.06(6); O(4)−P(1)−O(1), 109.73(6); O(2)−P(1)−P(4), 110.46(6); O(3)−P(1)−O(1), 109.82(6).

Received: May 14, 2015
Published: June 4, 2015

DOI: 10.1021/acs.orglett.5b01414
Org. Lett. 2015, 17, 3114−3117

and O4, at the terminal positions are almost equal (P1−O3 = 1.467(1) and P1−O4 = 1.478(1) Å) and much shorter than those from the phenoxy oxygen (P1−O1 = 1.621(1) and P1−O2 = 1.638(1) Å). The P−O bond distances indicate the delocalized anionic state of the phosphate unit. These facts strongly suggest the zwitterionic structure of **1** in the crystal.

The positions of the two N−H protons were determined by the difference Fourier synthesis and optimized. One of the pyrrole N−H protons is involved in an intramolecular hydrogen bond with the O1 atom (O1···H = 1.99 Å, O1···N1 = 2.609(2) Å, ∠O1−H−N1 = 124.5°). The other N−H proton is close to the O4* atom of the other molecule, which indicates the intermolecular hydrogen bond (O4···H = 1.78 Å, O4···N2* = 2.674(2) Å, ∠O4−H−N2* = 158.2°). The hydrogen bonds with the anionic phosphate unit should stabilize the protonated state of the dipyrrin. In the reported structures of protonated dipyrrin-phosphate adducts, a similar hydrogen bond between the N−H and P−O units was shown.[14]

The UV−vis absorption and fluorescence spectra of **1** in 1:10 $CH_3OH/CHCl_3$ (v/v) showed two maxima (542 and 590 nm in UV−vis, 566 and 615 nm in fluorescence). Protonated **1** was expected to have acid/base responsive properties. In fact, upon the addition of triethylamine (TEA), the short-wavelength absorption maximum in the initial state increased and the long one decreased with the isosbestic points (Figure 2a). These facts imply equilibrium between **1** and deprotonated **1′** in solution (Scheme 2).

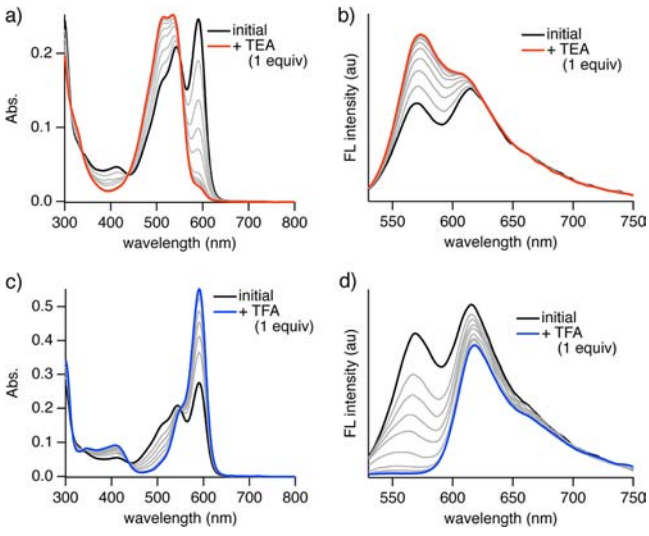

Figure 2. UV−vis absorption and fluorescence spectroscopic titration of **1** with TEA (a and b) and TFA (c and d) (1:10 $CH_3OH/CHCl_3$, 10 μM, λ_{ex} = 520 nm).

Scheme 2

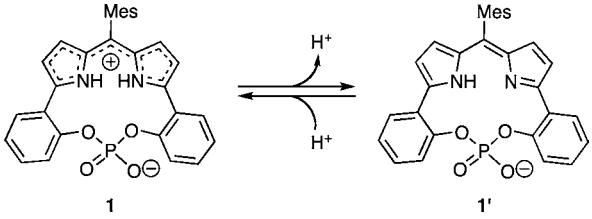

In the fluorescence spectra, the short-wavelength fluorescence increased (Figure 2b). Thus, the absorption and fluorescence bands at the higher energy are assigned to those of the deprotonated form **1′**. On the other hand, the long-wavelength absorption and fluorescence increased upon the addition of TFA as the equilibrium moved to the protonated form **1** (Figure 2c and d). The protonated dipyrrins often show more red-shifted absorption and fluorescence than the nonprotonated ones.[8,15] The consecutive protonation/deprotonation of **1** with acid/base can be repeated without decomposition of the compound (Supporting Information Figure S7 and S8). In the absence of an acid and base, the ratio of [**1**]/[**1′**] was estimated by a curve-fitting method to be 1.39. The spectrum simulated by the analysis was very close to the observed one (Supporting Information Figure S6).

To clarify the electronic structure, a time-dependent (TD) DFT calculation was performed on the model structure of **1** and **1′** without the *meso*-mesityl group at the M062X/6-311G++(2d,p)//M062X/6-31++G(d,p) level. The shapes of the Kohn−Sham frontier orbitals of **1** and **1′** are very similar to each other (Supporting Information Figure S14). The S_1 states of both compounds correspond to HOMO−LUMO transition with >95% contribution. The S_1-state excitation energy of **1′** is higher than that of **1** (Figure 3). Thus, the red shifts of the protonated **1** should be due to the decrease in the excitation energy.

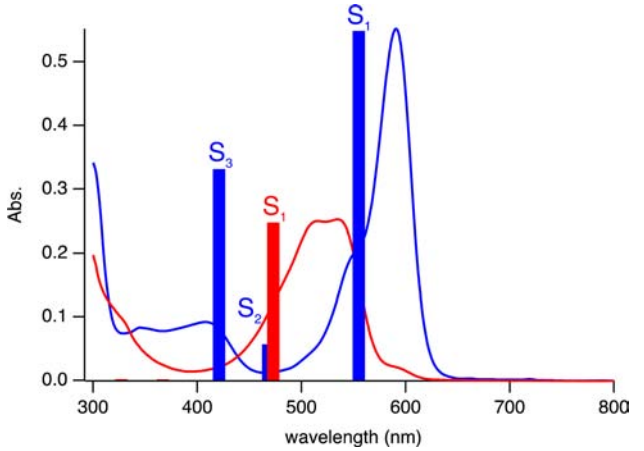

Figure 3. UV−vis absorption spectrum of **1** (blue line) with TFA (1 equiv) and (red line) with TEA (1 equiv) (10 μM, 1:10 $CH_3OH/CHCl_3$). The excitation energy calculated by TD DFT at the M062X/6-311G++(2d,p)//M062X/6-31++G(d,p): (blue bar) a model of **1** and (red bar) a model of **1′**·H^+.

The proton response of **1** was further confirmed by ^{1}H NMR spectroscopy. In the ^{1}H NMR spectra of **1** in 1:10 $CD_3OD/CDCl_3$, all the signals are broadened (Figure 4a). The signals shifted upfield upon the addition of TEA (Figure 4b), while they shifted downfield upon the addition of TFA (Figure 4c). These facts support the interconversion between **1** and **1′** that causes the downfield and upfield shifts of the protons in an aromatic region according to the protonation and deprotonation of the dipyrrin unit, respectively.

The absorption spectra of **1** in an aqueous saline solution (5:95 DMSO/PBS) showed a sharp signal (Supporting Information Figure S9). In the fluorescence spectra of the solution of **1** (Figure 5), a weak peak at 610 nm, which is assigned to **1**, was observed at a lower pH (2−4). As the pH

DOI: 10.1021/acs.orglett.5b01414
Org. Lett. 2015, 17, 3114−3117

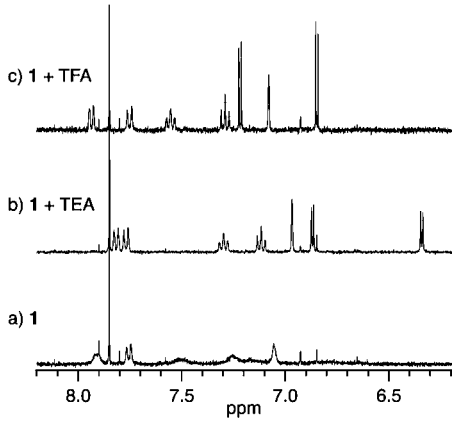

Figure 4. ^{1}H NMR spectra of **1** with (a) none, (b) TEA (1 equiv), or (c) TFA (1 equiv) (400 MHz, $[\mathbf{1}]_0$ = 1.0 mM, 1:10 $CD_3OD/CDCl_3$ (v/v)).

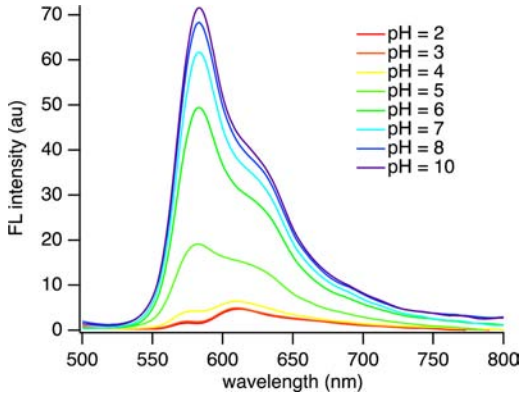

Figure 5. Fluorescence spectra of **1** at different pH values (5:95 DMSO/PBS buffer, 10 μM, [PBS] = 20 mM, [NaCl] = 100 mM, λ_{ex} = λ_{max} (absorption)).

value is greater than 5, the fluorescence wavelength was shifted to the blue-region (λ_{max} = 575 nm). The fluorescence intensity at 575 nm increased to undergo a 25-fold change at pH = 11 (Φ = 1.5%). Thus, the deprotonated form **1′** is emissive in aqueous media. A nonlinear least-squares analysis of the absorption change afforded the pK_a value of **1** to be 5.8. In contrast, the fluorescence of the dipyrrin **2** (Scheme 3) was

Scheme 3

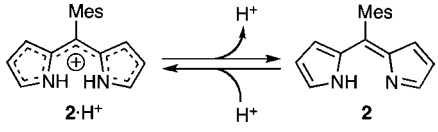

negligibly weak in all the pH ranges (2−11) (Supporting Information Figure S11). An excited state of **2** might be deactivated via a nonemissive process by the hydrogen bond of **2** with the solvent water or rotation of the pyrrole ring. The rigid cyclic structure of **1′** presumably results in the significant fluorescence even in aqueous media. The pK_a value of **2**·H$^+$ was determined to be 7.2 (Supporting Information Figure S10), much higher than that of **1**. The distortion between the two pyrrole rings probably more destabilizes the protonated form **1**, and **1** was thought to be more easily deprotonated than **2**·H$^+$.

The pK_a value of **1**, 5.8, is significantly important for application to bioimaging because Nagano and his colleagues reported an optimum pK_a level in pH-responsive fluorescence probes for tumor cell imaging.[6] They concluded that probe "DiEtN-BDP" (pK_a = 5.8−6.0) is the best agent for in vivo tumor imaging. We examined the in vitro pH response of **1** in living cells. HeLa cells, that is, human female cervix tumor cells, were treated with **1** under acidic (pH = 5.0) or basic (pH = 8.0) conditions, and then orange-colored fluorescence in the cells was observed (Supporting Information Figure S12).

The fluorescence microscope images of the stained cells were collected over 500 nm. The fluorescence images showed a sufficient cellular uptake of **1** and distinct pH-responsive fluorescence of **1** in the cells (Figure 6). The pH-response

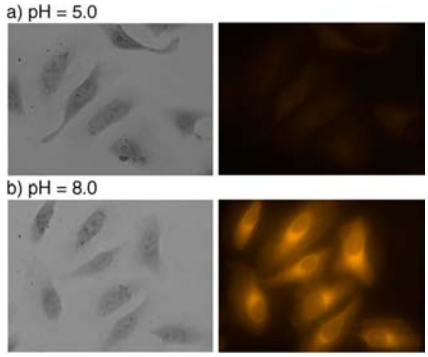

Figure 6. Optical (left) and fluorescence (right) microscope images of HeLa cells treated with **1** (20 μM, 10 min) under (a) acidic (pH = 5.0) and (b) basic (pH = 8.0) conditions (1:99 DMSO/PBS buffer, [PBS] = 20 mM). The fluorescence images were collected over 500 nm when a high-pressure mercury lamp was irradiated through a 460−490 nm dichromic filter.

using the probe **1** is conveniently observed even with the naked eye. The pH-responsive fluorescence was reversibly visualized by alternately changing the pH value of buffer between 5.0 and 8.0 (Supporting Information Figure S13). This fact indicates that **1** should quickly respond to environmental pH in vivo.

In summary, the one-step reaction of the N_2O_2-type dipyrrin with phosphoryl chloride gave the zwitterionic protonated-dipyrrin **1** bearing the phosphate unit. Compound **1** is in equilibrium with the deprotonated form **1′** in solution and shows a significantly pH-responsive absorption and fluorescence. Compound **1** is soluble in aqueous media, and the fluorescence intensity increased as the pH value increased. The pK_a value of **1** is estimated to be 5.8 in aqueous media. In addition, the pH-responsive fluorescence of **1** was observed in living cells. These results indicate that the pH-responsive fluorophore **1** in aqueous media should be applicable as a pH probe for determining tumor cells from normal cells.

■ ASSOCIATED CONTENT

Supporting Information

Experimental details, spectral data, and crystallographic information. The Supporting Information is available free of charge on the ACS Publications website at DOI: 10.1021/acs.orglett.5b01414.

■ AUTHOR INFORMATION

Corresponding Author

*E-mail: nabesima@chem.tsukuba.ac.jp.

DOI: 10.1021/acs.orglett.5b01414
Org. Lett. 2015, 17, 3114−3117

Notes

The authors declare no competing financial interest.

■ ACKNOWLEDGMENTS

This research was financially supported by Grants-in-Aid for Scientific Research (Innovative Area: Stimuli-responsive Chemical Species) from the Ministry of Education, Culture, Sports, Science, and Technology of Japan. HeLa cell line (RCB0007) was provided by RIKEN BRC through the National Bio-Resource Project of the MEXT, Japan.

■ REFERENCES

(1) *Molecular Probes Handbook, A Guide to Fluorescent Probes and Labeling Technologies*, 11th ed.; Johnson, I., Spence, M. T. Z., Eds.; Life Technologies Corporation: Carlsbad,CA, 2010.
(2) Okamoto, C. T. *Adv. Drug Delivery Rev.* **1998**, *29*, 215.
(3) (a) Martinez-Zaguilln, R.; Gillies, R. J. *Cell Physiol. Biochem.* **1996**, *6*, 169. (b) Chiche, J.; Ilc, K.; Laferrière, J.; Trottier, E.; Dayan, F.; Mazure, N. M.; Brahimi-Horn, M. C.; Pouysségur, J. *Cancer Res.* **2009**, *69*, 358.
(4) Montcourrier, P.; Mangeat, P. H.; Valembois, C.; Salazar, G.; Sahuquet, A.; Duperray, C.; Rochefort, H. *J. Cell Sci.* **1994**, *107*, 2381.
(5) Overly, C. C.; Lee, K. D.; Berthiaume, E.; Hollenbeck, P. J. *Proc. Natl. Acad. Sci. U. S. A.* **1995**, *92*, 3156.
(6) Urano, Y.; Asanuma, D.; Hama, Y.; Koyama, Y.; Barrett, T.; Kamiya, M.; Nagano, T.; Watanabe, T.; Hasegawa, A.; Choyke, P. L.; Kobayashi, H. *Nat. Med.* **2009**, *15*, 104.
(7) Loudet, A.; Burgess, K. *Chem. Rev.* **2007**, *107*, 4891.
(8) La, J. Q.-H.; Michaelides, A. A.; Manderville, R. A. *J. Phys. Chem. B* **2007**, *111*, 11803.
(9) Boron and aluminum complexes: Ikeda, C.; Ueda, S.; Nabeshima, T. *Chem. Commun.* **2009**, 2544.
(10) Silicon, germanium, and tin complexes: (a) Sakamoto, N.; Ikeda, C.; Yamamura, M.; Nabeshima, T. *J. Am. Chem. Soc.* **2011**, *133*, 4726. (b) Nakano, K.; Kobayashi, K.; Nozaki, K. *J. Am. Chem. Soc.* **2011**, *133*, 10720. (c) Yamamura, M.; Takizawa, H.; Sakamoto, N.; Nabeshima, T. *Tetrahedron Lett.* **2013**, *54*, 7049. (d) Yamamura, M.; Albrecht, M.; Albrecht, M.; Nishimura, Y.; Arai, T.; Nabeshima, T. *Inorg. Chem.* **2014**, *53*, 1355.
(11) Weissleder, R.; Pittet, M. J. *Nature* **2008**, *452*, 580.
(12) Jiang, X.-D.; Zhao, J.; Xi, D.; Yu, H.; Guan, J.; Li, S.; Sun, C.-L.; Xiao, L.-J. *Chem.—Eur. J.* **2015**, *21*, 6079.
(13) The Cambridge Structural Database (CSD) was searched for dipyrrin derivatives. Except for a dipyrrin bearing crowded substituents, almost all dipyrrins adopt planar structure. Crowded dipyrrin, see: Li, J.; Hu, B.; Hu, G.; Li, X.; Lu, P.; Wang, Y. *Org. Biomol. Chem.* **2012**, *10*, 8848.
(14) (a) Iverson, B. L.; Shreder, K.; Král, V.; Sansom, P.; Lynch, V.; Sessler, J. L. *J. Am. Chem. Soc.* **1996**, *118*, 1608. (b) Král, V.; Lang, K.; Králová, J.; Dvořák, M.; Martásek, P.; Chin, A. O.; Andrievsky, A.; Lynch, V.; Sessler, J. L. *J. Am. Chem. Soc.* **2006**, *128*, 432.
(15) Melvin, M. S.; Tomlinson, J. T.; Park, G.; Day, C. S.; Saluta, G. R.; Kucera, G. L.; Manderville, R. A. *Chem. Res. Toxicol.* **2002**, *15*, 734.

DOI: 10.1021/acs.orglett.5b01414
Org. Lett. 2015, 17, 3114−3117